Available online at www.sciencedirect.com

ScienceDirect

Procedia Manufacturing 47 (2020) 1532–1539

Procedia MANUFACTURING

www.elsevier.com/locate/procedia

23rd International Conference on Material Forming (ESAFORM 2020)

Effect Of Temperature And Strain Rate On The Plastic Anisotropic Behavior Characterized By A Single Biaxial Tensile Test

Liang Jiabin[a], Guines Dominique[a] and Leotoing Lionel[a,*]

[a]*Univ. Rennes, INSA Rennes, LGCGM - EA 3913, F-35000 Rennes, France.*

* Corresponding author. Tel.: (33) 2 23238376; fax: (33) 2 23238726. *E-mail address: lionel.leotoing@insa-rennes.fr*

Abstract

The heterogeneous strain field measured by digital image correlation in the central gauge area of a cruciform specimen permits to characterize the plastic anisotropic behavior of metallic sheets with a unique specimen [1]. Indeed, minor and major strains measured along several paths show a wide range of strain states, from uniaxial to equi-biaxial stress state. Thanks to the recording of forces along the two loading directions and to the strain field measurement, an identification of complex anisotropic yield criteria (like Bron and Besson criterion) is possible by inverse procedure. Then, a unique test is sufficient to evaluate the anisotropic behavior of the sheet. The aim of this work is to evaluate the effect of temperature and strain rate on the anisotropic behavior of AA6061 sheet. For this purpose, a biaxial device equipped with four hydraulic cylinders and accumulators (applied speed until 200mm/s), and with an air flow generator (applied temperature up to 160°C) is used to perform in-plane biaxial tensile tests for different conditions of strain rate and temperature. Numerical simulations of the equi-biaxial tensile test are then performed for these different experimental conditions. The numerical simulations are based on a FE model of the cruciform specimen including temperature and strain rate hardening dependencies while the Bron and Besson yield criterion has been calibrated only at room temperature and under quasi-static conditions. Finally, agreement between experimental and numerical evolutions of principal strains and strain paths ratios along three specific profiles is compared and the relevance of using only one experimental condition (room temperature and quasi-static strain rate) to calibrate the yield criterion is discussed.

Keywords: Biaxial tensile test; Temperature; Strain rate; Anisotropic behavior

1. Introduction

In the characterization of plastic behavior for sheet metal forming, the consideration of temperature and strain effect is a crucial point. In literature, many works have been focused on the calibration of temperature and strain rate dependent hardening model. On the contrary, few studies concern the influence of both the strain rate and the temperature on anisotropic behavior.

Temperature influence on both hardening parameters and anisotropic coefficients for AA3001-H111 from 25°C to 260°C under very low strain rates (0.001-0.08s^{-1}) has been studied by Abedrabbo et al. [2]. Conclusion of this work is that the anisotropic coefficients must be determined as a function of temperature so that the material model can account the material response to loading conditions at elevated temperatures. On the other hand, through uniaxial tensile tests for TRIP steel along RD, TD and DD with a strain rate ranging from 0.005s^{-1} to 500 s^{-1}, Alturk et al. [3] investigated the strain rate influence on anisotropic coefficients *r*-values. They concluded that a rate-dependent anisotropic yield criterion is necessary for modeling the anisotropic behavior during the forming process. Khan et al. [4] has investigated the anisotropic behavior of AA5182-O at a range of temperatures (296K to 473K) and strain rates ($10^{-4}s^{-1}$ to $10^{0}s^{-1}$) using uniaxial tensile tests. The Khan-Liang hardening model with a strain rate and temperature dependency is identified on the whole temperature and strain rate ranges. For the anisotropic behavior, the parameters of the yield

10.1016/j.promfg.2020.04.346

criterion were obtained for each condition. Liu et al. [5] proposed a temperature-dependent yield function coupled with the Hockett-Sherby hardening model to describe the plastic behavior for AA5086-H111 for ambient temperature to 240°C. The anisotropic coefficient is determined with the others hardening parameters in function of equivalent plastic strain and temperature. The author concluded that, this temperature-dependent constitutive model well predict the anisotropic mechanical behavior of the considered material. This model gives better prediction for *r*-values compared to the Hill 48 yield criterion.

Compared with the conventional experimental test such as uniaxial tensile test, the in-plane biaxial tensile test on a cruciform specimen shows a particular advantage in the investigation of anisotropic behavior of materials. Zhang et al. [6] characterized the plastic anisotropic behavior of AA5086 with Bron and Besson yield criterion [7] through biaxial tension at room temperature. The researchers conclude that, compared with the conventional method, a single equi-biaxial tensile test is sufficient to identify the parameters for a complex yield criterion. Moreover, Zhang et al., through numerical analysis, showed that the prediction of the strain distribution in the central area of the specimen is dependent on the yield criterion selected.

In the last decade, several heating devices have been developed on biaxial testing machines [8,9,10,11]. But up today, very few studies concern the characterization of temperature and strain rate dependent anisotropic behavior under biaxial loadings.

The present paper aims to evaluate the effect of temperature and strain rate on the plastic anisotropic behavior of AA6061 submitted to biaxial loadings. The hardening model depending on temperature and strain rate influence is combined with Bron and Besson yield criterion to predict the principal strain along different paths of a dedicated cruciform specimen. Biaxial tensile tests for AA6061 are performed at tensile velocities of 1mm/s and 200mm/s with temperature ranging from ambient to 160°C. The parameters of the yield criterion are identified under a quasi-static tensile condition at room temperature. After that, the prediction of the anisotropy, identified at room temperature and for quasi-static condition, is discussed for the different tested conditions by means of comparisons between numerical and experimental results.

2. Identification strategy of an anisotropic yield criterion

The identification strategy of an anisotropic yield criterion for metallic sheet based on an unique equi-biaxial tensile test has been proposed by Zhang [6] through an inverse identification procedure. According to the proposed calibration method, the parameters of the complex yield model of Bron and Besson have been identified. Nevertheless, if the identified yield model can well describe the evolutions of principal strains along the considered diagonal profiles, significant discrepancies between predictions and experimental data can be observed for others profiles.

In order to improve the prediction, two additional profiles (along the longitudinal and transversal direction with respect to the rolling direction) have been added to the initial diagonal profile in the calibration procedure, as shown in Fig. 1. As one can see it, due to symmetries, the numerical finite element model of the biaxial tensile test is based on only one quarter of geometry of the tested specimen.

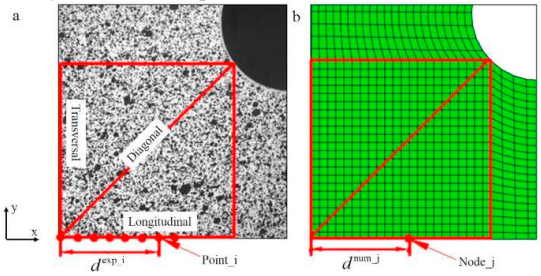

Fig. 1. (a) Experimental specified paths in the central part of the cruciform specimen ; (b) Mesh and numerical specified profiles considered in FE simulations.

The calibration process is performed using the modeFRONTIER software platform allowing the coupling between a FE simulation code (ABAQUS software) and optimization algorithms. The optimization process is based on the minimization of the cost function δ defined by the difference between numerical and experimental principal strains along the specified paths, as shown in the Eq. (1) below:

$$\delta_x = \sum_i^p \left(\frac{\varepsilon_{1,x}^{num\ i} - \varepsilon_{1,x}^{\exp i}}{\varepsilon_{1,x}^{\exp i}} \right)^2 + \sum_i^p \left(\frac{\varepsilon_{2,x}^{num\ i} - \varepsilon_{2,x}^{\exp i}}{\varepsilon_{2,x}^{\exp i}} \right)^2$$

$$\delta_y = \sum_i^p \left(\frac{\varepsilon_{1,y}^{numi} - \varepsilon_{1,y}^{\exp i}}{\varepsilon_{1,y}^{\exp i}} \right)^2 + \sum_i^p \left(\frac{\varepsilon_{2,y}^{numi} - \varepsilon_{2,y}^{\exp i}}{\varepsilon_{2,x}^{\exp i}} \right)^2 \quad (1)$$

$$\delta_{diag} = \sum_i^p \left(\frac{\varepsilon_{1,diag}^{numi} - \varepsilon_{1,diag}^{\exp i}}{\varepsilon_{1,diag}^{\exp i}} \right)^2 + \sum_i^p \left(\frac{\varepsilon_{2,diag}^{numi} - \varepsilon_{2,diag}^{\exp i}}{\varepsilon_{2,diag}^{\exp i}} \right)^2$$

$$\delta = \delta_x + \delta_y + \delta_{diag}$$

Where $\varepsilon_1^{\exp i}$ and $\varepsilon_2^{\exp i}$ are the experimental values for the major and minor strains respectively; ε_1^{numi} and ε_2^{numi} are the numerical major and minor principal strains, respectively; p is the number of strain calculation points along each profile.

3. Experimental characterization of AA6061

3.1. Experimental setups

Static and dynamic equi-biaxial tensile tests are performed on a specific experimental device equipped with four hydraulic actuators. Therefore, in order to investigate the temperature effect, the specimen is placed in an insulated box fed by a hot air generator, as shown in Fig. 2.

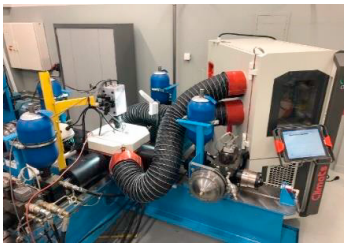

Fig. 2. Biaxial tensile machine equipped with the heating device.

Inside the insulated box, the temperature of the specimen is considered as homogeneous before the test. A high-resolution camera is placed on the top of the insulated box to record the deformation of the specimen during the test through the cover window. The main acquisition parameters of the camera are presented in Table 1. The shape of the cruciform specimen used in this study (Fig. 3) has been already validated by Zhang et al. [6].

Table 1 Main characteristics of image acquisition.

Tensile velocity	Camera		
	Image Resolution (pixel)	Acquisition rate (Fps)	Shuttle speed (s)
1 mm/s	1024 × 1024	250	1/800
200 mm/s	1024 × 1024	3000	1/3000

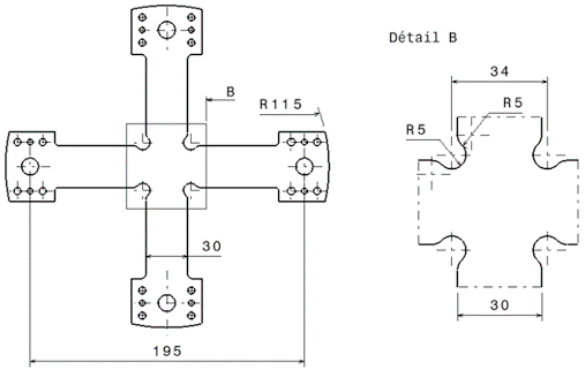

Fig. 3. Geometry of the cruciform specimen.

3.2. Experimental results

Three equi-biaxial tensile tests are carried out respectively at (1 mm/s; room temperature), (1 mm/s; 160 °C) and (200 mm/s; 160°). The tensile velocities given above are applied on each specimen arm.

The experimental forces are measured by load sensors on each axis of the specimen and presented in Fig. 4. In order to compare all the conditions, load versus displacement curves are plotted. The temperature effect is clearly shown between the two tests performed at 1 mm/s with respectively a maximum force of 15200 N and 12300 N at ambient and 160°C. A small strain rate effect is exhibited at the temperature of 160°C, where the maximum force reaches 12300 N and 13000 N, respectively at 1 mm/s and 200 mm/s, whereas no strain rate effect is observed at room temperature.

The principal strains at the surface of specimen for the different conditions are obtained by post-treatment with the DIC software GOM. Fig. 5 shows an image of the cruciform specimen at the initial state. The square area in blue line with a size of approximately $25\times25\text{mm}^2$ at the central gauge of specimen is selected to calculate the principal strains. The size of the facet is 32×32 pixels and the distance between each facet is 16 pixels. The blue square area is defined by (about $660\,pixels\times660\,pixels$) corresponding to 0.0378mm/pixel. The lines x1 and x2 correspond to the longitudinal profiles (rolling direction), y1 and y2 correspond to transverse profiles, and the lines 1 to 4 correspond to the diagonal profiles. The evolution of experimental principal strains according to the longitudinal, transverse and diagonal directions used in the calibration procedure of the yield criterion (Eq. (1)) is the average value for each direction, respectively.

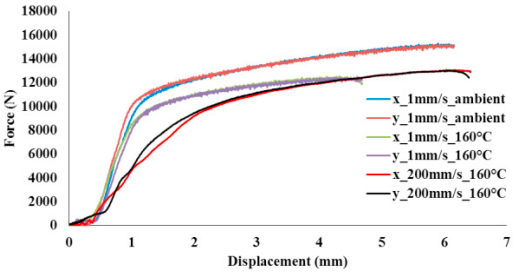

Fig. 4. Evolution of forces along each axis for different conditions.

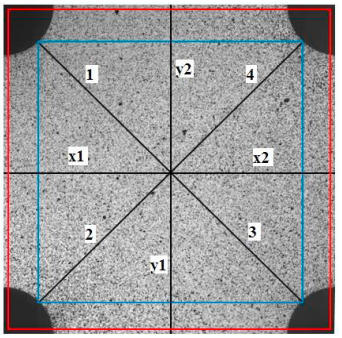

Fig. 5. Analysis areas and visualization of specified profiles.

Since the necking effect is not considered in this work, a time before the onset of necking is considered in this work. Fig. 6 shows the evolution of principal strains along all the profiles for the three directions (longitudinal, transverse or diagonal) at time t = 5s for the equi-biaxial tensile test carried out at (1 mm/s ; room temperature). The time at rupture for this testing condition is 6.16 s.

It can be seen that, for a considered direction (longitudinal, transverse or diagonal), the principal strains along each profile are very similar. It shows a good synchronization of the displacement imposed on each arm of the cruciform specimen.

For the other two conditions, the same method is performed on the strain measurement.

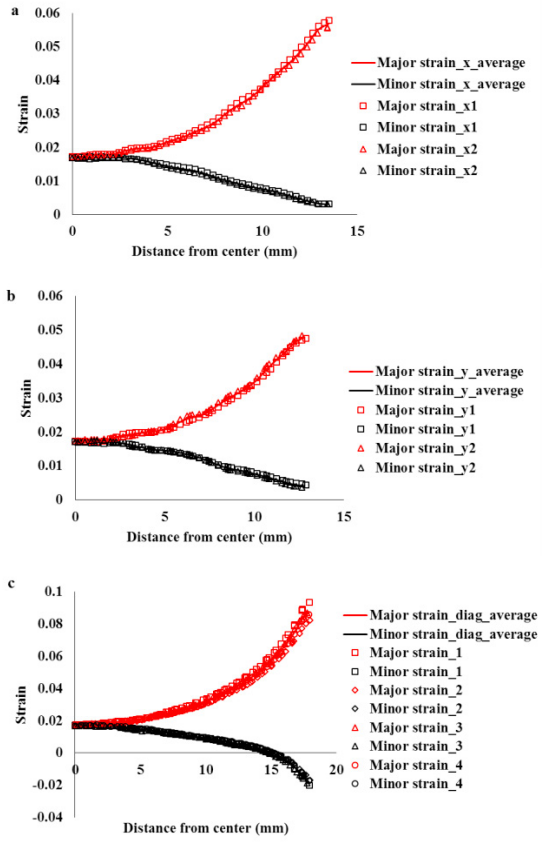

Fig. 6. Principal strain along different profiles for 1mm/s at ambient.
(a) longitudinal; (b) transverse; (c) diagonal.

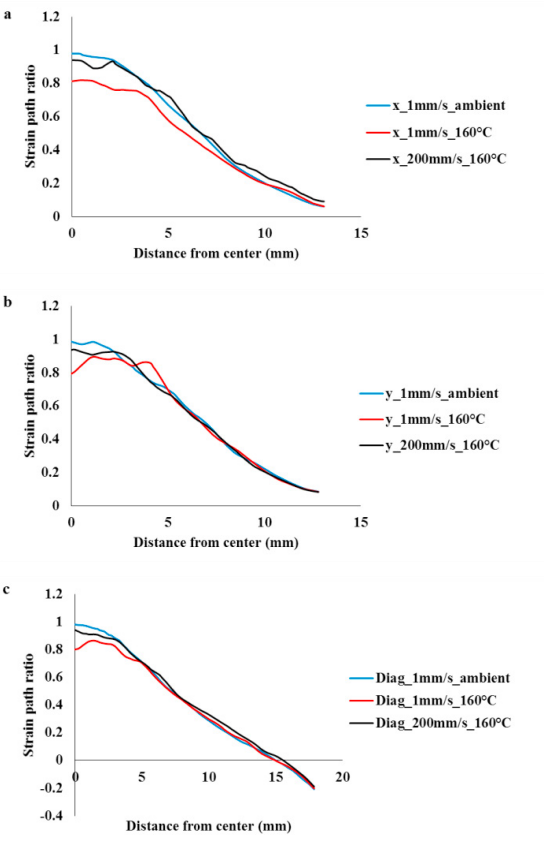

Fig. 7. Strain path ratios along different profiles for 1mm/s at 160°C.
(a) longitudinal; (b) transverse; (c) diagonal.

The evolution of strain path ratio, defined as the ratio $\varepsilon_2/\varepsilon_1$, is figured out with the average principal strains for each direction and presented in Fig. 7. It can be clearly seen that the strain path ratio at the central point of the specimen is closed to 1 (between 0.8 and 1) whatever the tested condition, which can be considered as an equi-biaxial tensile strain state. For the longitudinal and transverse directions, the strain state varies from the equi-biaxial tensile strain state to a plane strain state (0.08). For the diagonal direction, the strain state varies from an equi-biaxial tensile state to a state (about -0.2) between uniaxial tensile state (-0.3) and plane strain state (0).

4. Identification of anisotropic Bron & Besson yield criterion

Based on the method briefly explained in section 2, the Bron and Besson yield criterion is identified from the equi-biaxial tensile test performed at 1mm/s and room temperature. A uniaxial tensile test at room temperature and quasi-static strain rate along the rolling direction has been performed to calibrate the Voce hardening law (Eq. (2)). The calibrated parameters are presented in Table 2.

$$\bar{\sigma} = \sigma_s + k \cdot \left(1 - e^{-n \cdot \bar{\varepsilon}_p}\right) \tag{2}$$

Table 2. Identified parameters for Voce law.

σ_s (MPa)	k (MPa)	n
160.5	198.7	14.06

The function of Bron and Besson model can be written as:

$$\psi = \left(\sum_{k=1}^{2} \alpha^k \left(\bar{\sigma}^k \right)^a \right)^{1/a} \tag{3}$$

α^k are positive coefficients, and $\alpha_1 + \alpha_2 = 1$. The $\bar{\sigma}^k$ are expressed in the form:

$$\bar{\sigma}^1 = \left[\frac{1}{2} \left(\left| S_2^1 - S_3^1 \right|^{b_1} + \left| S_3^1 - S_1^1 \right|^{b_1} + \left| S_2^1 - S_1^1 \right|^{b_1} \right) \right]^{1/b_1}$$
$$\bar{\sigma}^2 = \left[\frac{3b_2}{2^{b_2} + 2} \left(\left| S_1^2 \right|^{b_2} + \left| S_2^2 \right|^{b_2} + \left| S_3^2 \right|^{b_2} \right) \right]^{1/b_2} \tag{4}$$

In these equations, a, b_1, b_2 and α_k are parameters which define the shape of the yield surface. S_i^k are the principal values of transformed stress deviators $s_{ij}'^k$ which were defined by :

$$s'^{k}_{ij} = L^{k}\sigma_{ij}$$

$$L^{k} = \begin{Bmatrix} \frac{c_2^k + c_3^k}{3} & -\frac{c_3^k}{3} & -\frac{c_2^k}{3} & 0 & 0 & 0 \\ -\frac{c_3^k}{3} & \frac{c_1^k + c_3^k}{3} & -\frac{c_1^k}{3} & 0 & 0 & 0 \\ -\frac{c_2^k}{3} & -\frac{c_1^k}{3} & \frac{c_1^k + c_2^k}{3} & 0 & 0 & 0 \\ 0 & 0 & 0 & c_4^k & 0 & 0 \\ 0 & 0 & 0 & 0 & c_5^k & 0 \\ 0 & 0 & 0 & 0 & 0 & c_6^k \end{Bmatrix} \quad (5)$$

c_i^k are the parameters related to anisotropy of the material. In plane stress conditions, the parameter number related to anisotropy reduces down to 8 with $c_5^k = c_6^k = 1$.

The identified parameters of the Bron and Besson criterion are presented in Table 3. Figure 8 shows the yield contour obtained with these parameters. In this figure, Mises yield surface is also given as a comparison. The prediction of principal strains and strain path ratios for Bron and Besson are compared with the prediction of Von-Mises model and experimental data, as presented in Fig. 9 and Fig. 10, respectively. It can be seen that, compared with the isotropic model, the anisotropic one gives a better description of strain evolution and strain path ratio along different directions.

Only for Bron and Besson model, the principal strains at the central point present a good match between the predictions and experimental data for all the conditions. When moving away from the center of the specimen, small discrepancies appear between the predicted and experimental principal strains depending on the profile considered. Experimental and predicted major and minor strains are in very good agreement along the longitudinal direction. For the transverse and diagonal direction, the predicted major strain curves underestimate the experimental ones and a small difference can be observed. While for the evolution of minor strain along these two transverse and diagonal directions are quite good.

Considering the strain path ratios, good agreement is obtained between experimental and predicted results for the longitudinal and diagonal directions, while some discrepancies are observed for the transverse direction.

Table 3. Identified parameters for Bron and Besson yield criterion.

α_1	a	b_1	b_2	c_1^1	c_2^1
0.763	0.527	11.804	12.55	0.71	0.65
c_3^1	c_4^1	c_1^2	c_2^2	c_3^2	c_4^2
0.271	0.431	0.296	0.434	1.104	0.548

5. Sensitivity to temperature and strain rate for plastic behavior

Non-dependent temperature and strain rate elastic parameters E=63240 MPa and ν=0.33 are considered for AA6061. The thermal properties adopted here has been presented in [12].

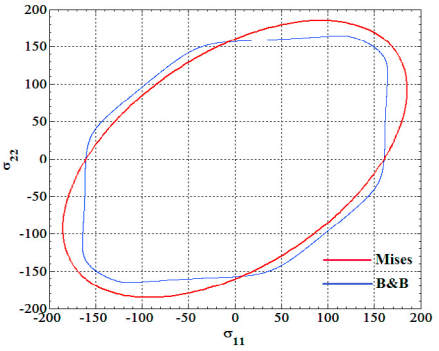

Fig. 8. Comparison of Bron and Besson and Mises yield contours.

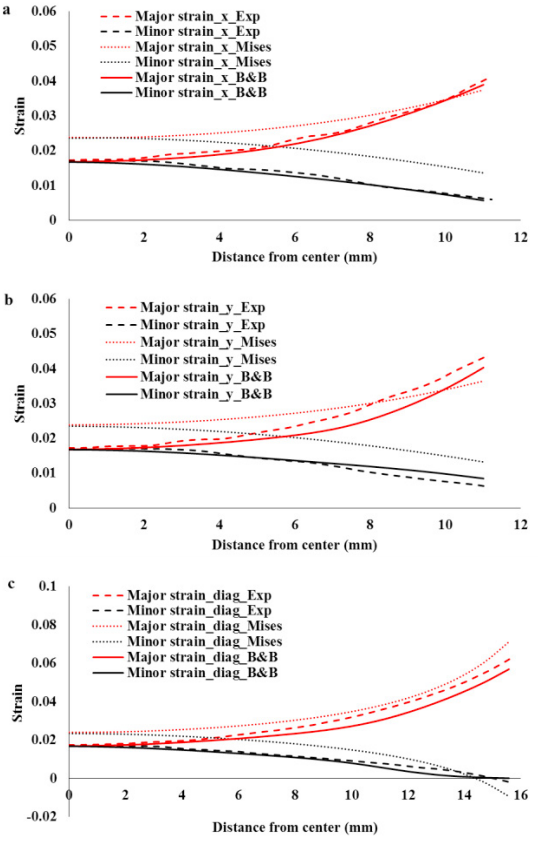

Fig. 9. Experimental and predicted principal strains along three profiles at 1mm/s and room temperature: (a) longitudinal; (b) transverse; (c) diagonal.

5.1. Temperature and strain rate dependent hardening model

A temperature and strain rate dependent hardening model (Voce type) has been calibrated from uniaxial tensile tests carried out in the same range of temperature and strain rate than those considered here. The formulation of the hardening law is:

$$\bar{\sigma} = \sigma_0(T) + K_1 e^{-K_2 T}\sqrt{1 - e^{-K_3 e^{K_4 T}\bar{\varepsilon}_p}}\,\dot{\bar{\varepsilon}}^{m_0 e^{m_1 T}} \quad (6)$$

With

$$\sigma_0(T) = \left[1 - \frac{T}{T_m} e^{K_0\left(1-\frac{T_m}{T}\right)}\right] \cdot \sigma_0(T_0) \quad (7)$$

As in Eq. (2), the initial yield stress $\sigma_0(T_0)$ = 160.5MPa at room temperature. The identified parameters are presented in Table 4. The hardening law plotted for different temperatures and strain rates are shown in Fig 11.

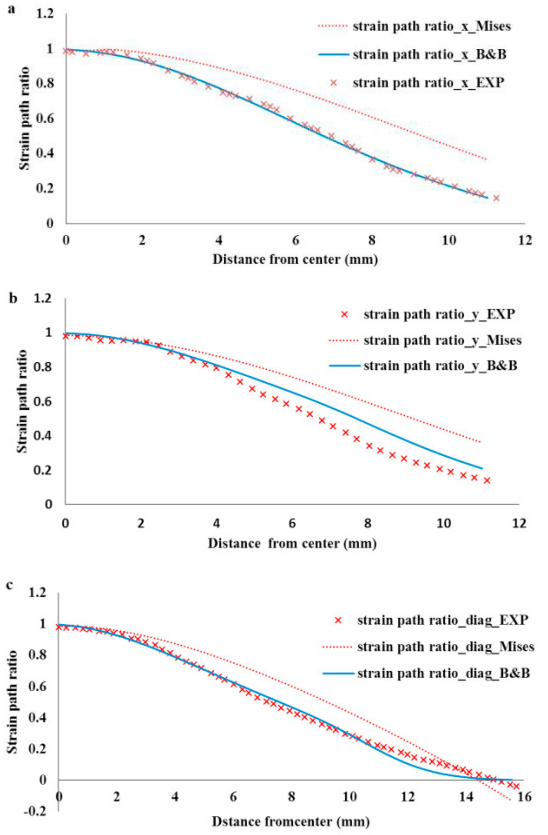

Fig. 10. Experimental and predicted strain path ratio along three profiles at 1mm/s and room temperature : (a) longitudinal; (b) transverse; (c) diagonal.

This temperature and strain rate dependent hardening law is then combined with the identified Bron and Besson yield criterion to discuss the temperature and strain rate influences on the anisotropic plastic behavior of AA6061.

Table 4. Parameters of hardening law.

$K_1(MPa)$	$K_2(^\circ C^{-1})$	K_3	$K_4(^\circ C^{-1})$
334.2	0.003065	2.2931	0.006332
m_0	$m_1(^\circ C^{-1})$	T_m	K_0
0.005643	0.008106	617.0	0.359

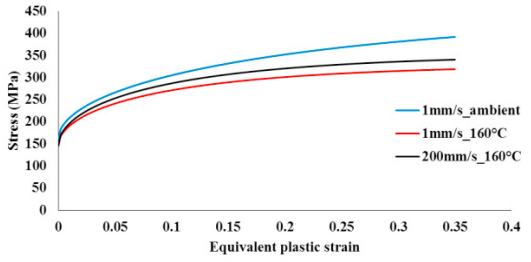

Fig. 11. Comparison of hardening law for three conditions

5.2. Comparison between numerical simulation results and experimental data

The experimental forces measured for the experimental equi-biaxial tensile tests at 1mm/s and 200mm/s for a temperature of 160 °C are imposed as boundary conditions in the FE model of the equi-biaxial tensile test.

Predicted principal strains and strain path ratios along longitudinal, transverse and diagonal profiles are compared with experimental data (Fig. 12 to Fig. 15).

For the condition of 160°C at different tensile velocity, a significant discrepancy is observed for the profile along the three direction.

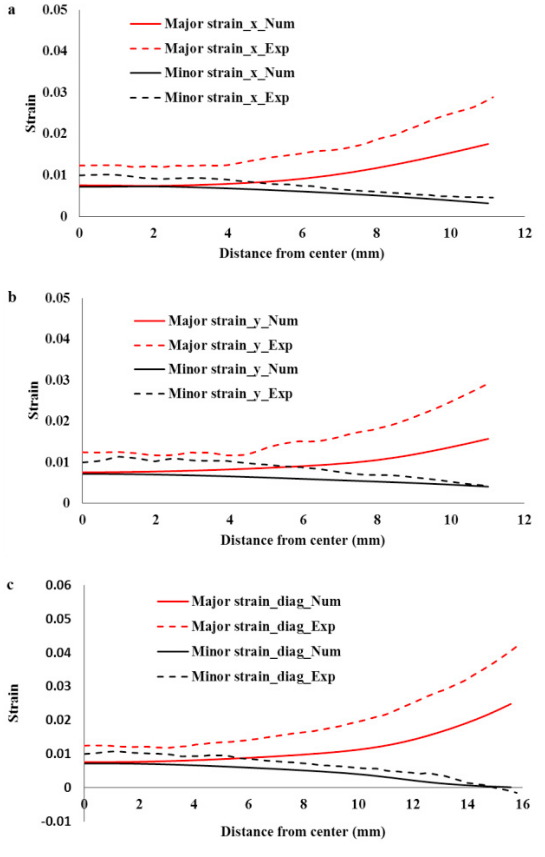

Fig. 12. Experimental and predicted principal strains along three profiles at 1mm/s, 160°C. (a) longitudinal ; (b) transverse ; (c) diagonal.

For the tensile velocity of 1mm/s (Fig. 12), the prediction of major strain shows an underestimation of around 30% compared to the experimental values. For the minor strain, the values at the center are quite close to the major strain, which also leads to an underestimation of 20%. With the increasing of distance, the discrepancy of minor strain become smaller. The predicted strain path ration at the center point is 0.95 which is higher than the experimental one (0.8). With the increasing of distance, the curves of prediction and experiment are getting close.

For the tensile velocity of 200mm/s (Fig. 14), the prediction of major strain show an underestimation around 40% compared to the experimental values. For the minor strain, the prediction leads to an underestimation of 30% at the center point. The predicted strain path ratio have a good agreement with the experimental results for this condition.

Based on these results, it can be assumed that this underestimation of the principal strain evolutions comes either from the parameters of the hardening model and/or those of the plastic criterion.

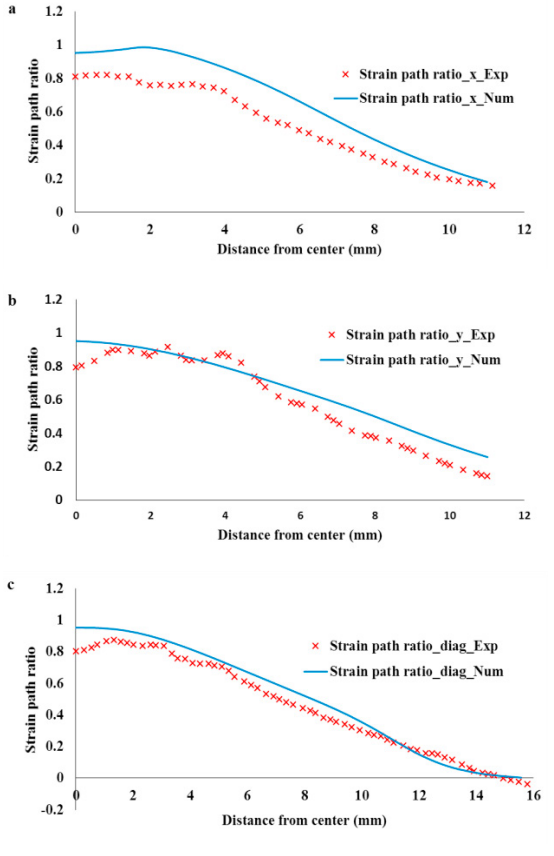

Fig. 13. Experimental and predicted strain path ratios along different profiles at 1mm/s, 160°C. (a) longitudinal ; (b) transverse ; (c) diagonal.

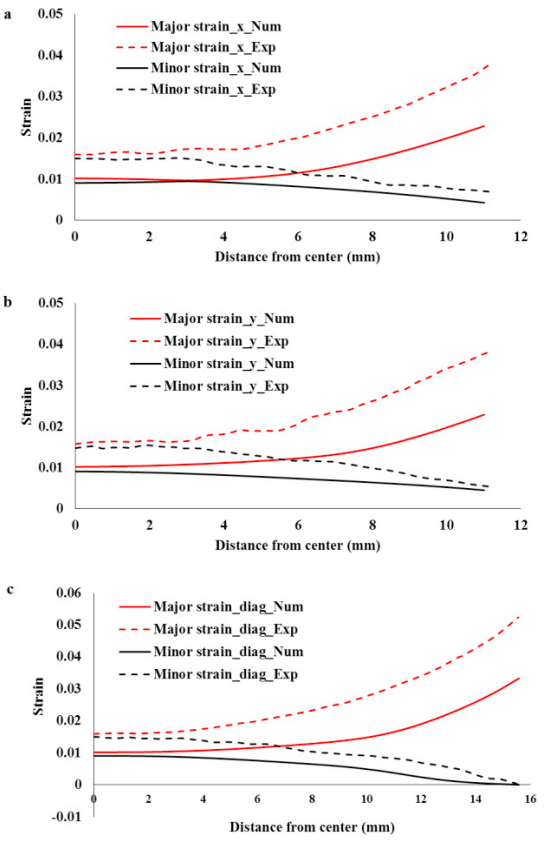

Fig. 14. Experimental and predicted principal strains along different strain profiles at 200mm/s, 160°C. (a) longitudinal ; (b) transverse ; (c) diagonal.

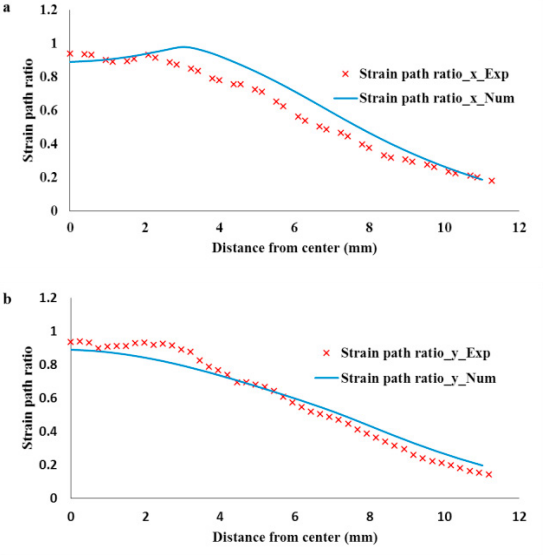

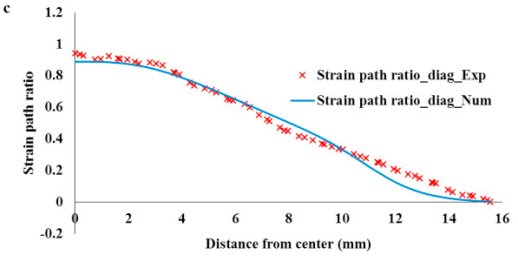

Fig. 15. Experimental and predicted of strain path ratios along different profiles at 200mm/s, 160°C. (a) longitudinal ; (b) transverse ; (c) diagonal.

6. Conclusion

Bron and Besson yield model has been adopted to predict the anisotropic behavior of material AA6061. Parameters of this yield function are obtained by minimizing the difference between experimental and numerical principal strains along three profiles (diagonal, longitudinal and transversal) defined in the central area of the cruciform specimen. Only one equi-biaxial tensile test under quasi-static tensile velocity condition and room temperature has been used to calibrate the complex Bron and Besson yield criterion. Results show that this anisotropic yield model well described the strain field of in the central area of the specimen for AA6061 for quasi-static condition at room temperature.

Nevertheless, the comparison of the principal strains along different profiles of the specimen central area shows significant differences at 160°C for both tensile velocities of 1mm/s and 200mm/s when the dependency of the strain rate and the temperature are taken into account only on the strain hardening and not on the anisotropic behavior of the material. So, to improve the prediction, it seems necessary to consider the temperature and/or the strain rate influence for the calibration of the parameters of the anisotropic plastic criterion.

Another way for improvement of the prediction would also be to identify viscoplastic strain-hardening directly on the equi-biaxial test.

References

[1] Zhang S, Léotoing L, Guines D, Thuillier S. Potential of the Cross Biaxial Test for Anisotropy Characterization Based on Heterogeneous Strain Field. Exp Mech 2015;55:817–35.

[2] Abedrabbo N, Pourboghrat F, Carsley J. Forming of aluminum alloys at elevated temperatures – Part 1: Material characterization. Int J Plast 2006;22:314–41.

[3] Alturk R, Hector LG, Matthew Enloe C, Abu-Farha F, Brown TW. Strain Rate Effect on Tensile Flow Behavior and Anisotropy of a Medium-Manganese TRIP Steel. JOM 2018;70:894–905.

[4] Khan AS, Baig M. Anisotropic responses, constitutive modeling and the effects of strain-rate and temperature on the formability of an aluminum alloy. Int J Plast 2011;27:522–38.

[5] Liu W, Chen BK, Pang Y. A new temperature-dependent anisotropic constitutive model for predicting deformation and spring-back in warm deep drawing of automotive AA5086-H111 aluminium alloy sheet. Int J Adv Manuf Technol 2018;97:3407–21.

[6] Zhang S, Leotoing L, Guines D, Thuillier S, Zang S. Calibration of anisotropic yield criterion with conventional tests or biaxial test. Int J Mech Sci 2014;85:142–51.

[7] Bron F, Besson J. A yield function for anisotropic materials Application to aluminum alloys. Int J Plast 2004;20:937–63.

[8] Chevalier L, Marco Y. Identification of a strain induced crystallisation model for PET under uni-and bi-axial loading: Influence of temperature dispersion. Mech Mater 2007;39:596–609.

[9] Kulawinski D, Henkel S, Holländer D, Thiele M, Gampe U, Biermann H. Fatigue behavior of the nickel-base superalloy WaspaloyTM under proportional biaxial-planar loading at high temperature. Int J Fatigue 2014;67:212–219.

[10] Shao Z, Li N, Lin J, Dean TA. Development of a new biaxial testing system for generating forming limit diagrams for sheet metals under hot stamping conditions. Exp Mech 2016;56:1489–1500.

[11] Xiao R, Li X-X, Lang L-H, Chen Y-K, Yang Y-F. Biaxial tensile testing of cruciform slim superalloy at elevated temperatures. Mater Des 2016;94:286–294.

[12] Liang J, Guines D, Léotoing L. Thermo-viscoplastic behavior of AA6061 under dynamic biaxial loadings. AIP Conf. Proc., vol. 2113, AIP Publishing LLC; 2019, p. 180014.